

Thermocouple frequency response compensation leads to convergence of the surface renewal alpha calibration



T.M. Shapland^a, R.L. Snyder^b, K.T. Paw U^b, A.J. McElrone^{a,c,*}

^a Department of Viticulture & Enology, University of California, Davis, CA 95616, USA

^b Atmospheric Science, University of California, Davis, CA 95616, USA

^c United States Department of Agriculture-Agricultural Research Service, Crops Pathology and Genetics Research Unit, Davis, CA 95616, USA

ARTICLE INFO

Article history:

Received 12 August 2013

Received in revised form

17 December 2013

Accepted 7 January 2014

Keywords:

Coherent structures

Response time

Sensible heat flux density

Spectral attenuation

Structure function

Temperature ramps

ABSTRACT

Ramp-like shapes in the turbulent scalar trace are the signature of coherent structures, and their characteristics (i.e., amplitude and duration) are resolved via a structure-function model for use in the surface renewal flux calculation. The potential for surface renewal to provide inexpensive sensible heat flux measurements has not been fully realized because this method has required calibration against eddy covariance or other more expensive flux measurement techniques. The calibration factor alpha is ideally 0.5, but a broad range of values have been reported in the surface renewal literature. Although it has been hypothesized that the sensor size, and hence sensor frequency response characteristics, influence alpha, no effort has been previously made to compensate the thermocouple signal in surface renewal measurements. We evaluate methods for compensating the frequency response of a thermocouple in the time domain and the frequency domain, and we present a novel method for compensation in the lag domain (i.e., compensating the structure function directly). We evaluated the compensation procedure as it affects the resolution of ramp characteristics at both the smallest and the second smallest scales of ramp-like turbulent shapes. The surface renewal sensible heat flux estimates from the compensated robust thermocouples (76 μm diameter wire) agree well with the estimates from the compensated fragile thermocouples (13 μm diameter). Using both the data collected for the present experiment and a meta-analysis of data in the surface renewal literature, we correct the surface renewal estimates for thermocouple frequency response characteristics to obtain alpha calibrations that converge to close to the predicted value of 0.5. We conclude that the frequency response characteristics of the thermocouple are the prevailing influence on the alpha calibrations reported in the literature.

© 2014 Published by Elsevier B.V.

1. Introduction

Thermal inertia associated with thermocouple heat capacity attenuates the high frequency components of a measured temperature signal. The frequency response characteristics of fine-wire thermocouples can be compensated using time constants (e.g., Scadron and Warshawsky, 1952; Ballantyne and Moss, 1977) based on semi-empirical heat-transfer laws for cylindrical and spherical bodies immersed in turbulent fluid environments (King, 1914; Collis and Williams, 1959). Eddy covariance methodology has previously adopted the thermocouple frequency response compensation (Moore, 1986), but the application of the compensation

for surface renewal sensible heat flux estimation has not been investigated.

Surface renewal is an inexpensive alternative to eddy covariance for measuring sensible heat flux density because it requires only a fast-response air temperature sensor (Paw U et al., 1995). Ramp-like shapes in turbulent air temperature time series data are the signature of the coherent structures that dominate surface-layer energy and mass exchange (e.g., Gao et al., 1989). The amplitude and period of the ramps are resolved using the Van Atta (1977) structure function procedure and can be used to calculate the sensible heat flux density in the surface renewal paradigm (Paw U et al., 1995; Spano et al., 1997a). Surface renewal flux measurements, however, require calibration to account for the linear bias in the data (Paw U et al., 1995). The calibration factor alpha is obtained from the slope of the regression forced through the origin of a standard for sensible heat flux (generally taken as eddy covariance measurements) versus un-calibrated surface renewal sensible heat flux measurements. It is hypothesized that the alpha calibration accounts for the uneven heating within the coherent structure that arises from the non-uniform vertical distribution of heat sources in the plant

* Corresponding author at: Department of Viticulture & Enology, University of California, Davis, CA 95616, USA. Tel.: +1 530 754 9763; fax: +1 530 752 0382.

E-mail addresses: tmshapland@ucdavis.edu (T.M. Shapland), rlsnyder@ucdavis.edu (R.L. Snyder), ktpawu@ucdavis.edu (K.T. Paw U), ajmcelrone@ucdavis.edu (A.J. McElrone).

canopy (Paw U et al., 1995). Assuming a linear decrease in heating from the canopy top to the ground, where no heating occurs, Paw U et al. (1995) predicted an alpha calibration of 0.5. However, a broad range of alpha calibrations has been reported in the surface renewal literature over a variety of surfaces, instrumentation, experimental design, and processing scheme (e.g., Paw U et al., 1995, 2005; Snyder et al., 1996; Spano et al., 1997a, 2000; Chen et al., 1997b). As a result, it has been hypothesized that the alpha calibration also accounts for other physical processes, such as sensor frequency response characteristics (Paw U et al., 1995), micro-scale advection (Paw U et al., 1995), the coherent structure microfront duration and its impact on ramp resolution models (Chen et al., 1997a), effective coherent structure dimensions (Spano et al., 1997a; Chen et al., 1997b), and embedded, multiple scales (Shapland et al., 2012a,b).

Compared to finer diameter (13 and 25 μm) thermocouples, the relatively large 76 μm diameter sensors are more rugged, and therefore are more convenient for field experiments despite their slower response times. Duce et al. (1997) demonstrated a reduction in the magnitude of the surface renewal flux estimation when the air temperature data were collected using 76 and 25 μm diameter thermocouples compared to 13 μm diameter thermocouples. The results of this study varied by structure function time lag and the authors did not attempt to compensate the thermocouple signal. Even if Duce et al. (1997) had compensated the thermocouple signal, the structure function time lag effect may have made it difficult to draw conclusions about the compensation procedure. Chen et al. (1997a) identified the structure function time lag associated with the coherent structure microfront duration as the appropriate time lag for resolving ramp characteristics from data with a single ramp scale, and Shapland et al. (2012a) identified the structure function time lags for resolving ramp characteristics from data with two ramp scales. These developments have made it possible to characterize and correct the underestimation of surface renewal sensible heat flux density estimates due to high-frequency signal attenuation.

We investigate in this paper the accuracy of different approaches to determining the time constant and compensating the thermocouple signal for the resolution of air temperature ramp characteristics and estimation of surface renewal sensible heat flux. Time constants based on the measured thermocouple wire diameter and the mean wind velocity accurately compensate the signal, yielding the dimensions of both the small-scale embedded ramps (i.e., Scale One; Shapland et al., 2012a) and the larger scale ramps (Scale Two). We develop new methods for compensating the structure function directly and for estimating the ramp signal to noise ratio. Using data collected over bare soil and a sorghum canopy with thermocouples of various sizes and by performing a meta-analysis of the surface renewal literature, we demonstrate that the alpha calibration converges to close to its theoretically predicted value of 0.5 once the surface renewal measurements have been compensated for thermocouple frequency response characteristics.

2. Theory

2.1. Surface renewal and structure function analysis

In the surface renewal paradigm, the amplitude and period of the ramp-like patterns in scalar turbulence data are used to calculate the scalar flux density (Paw U et al., 1995). For example, the sensible heat flux density is calculated as follows:

$$H_{SR} = \alpha z \rho C_p \frac{a}{(d+s)} \quad (1)$$

where H_{SR} is the surface renewal sensible heat flux (W m^{-2}), α is the alpha calibration, z is the measurement height (m), ρ is the density of air (kg m^{-3}), C_p is the specific heat of air ($\text{J K}^{-1} \text{kg}^{-1}$), ramp

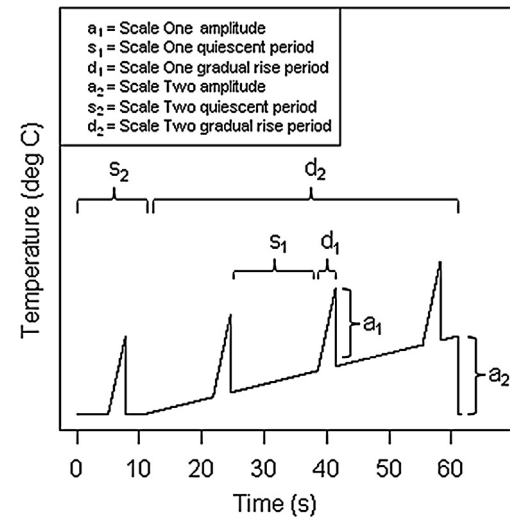


Fig. 1. A two-scale ramp model with an intermittent Scale One (smaller scale) ramp.

amplitude, a is the temperature ramp amplitude (K), d is the gradual rise period (s) of the temperature ramp, s is the quiescent period (s) of the temperature ramp, and the temperature ramp period ($d+s$) (s) is the sum of the gradual rise period and the quiescent period. Shapland et al. (2012a,b) expanded the original surface renewal concept of only one scale of turbulent scalar ramps to more than one scale (Fig. 1).

The Van Atta (1977) structure function procedure is used to resolve the ramp characteristics for the surface renewal calculation (Spano et al., 1997a; Shapland et al., 2012a,b). The structure function is the mean value of the time difference of a scalar taken to some power.

$$\overline{S^n(r)} = \frac{1}{L} \int_0^L [T(t) - T(t-r)]^n dt \quad (2)$$

where $\overline{S^n(r)}$ is the n th-order structure function, L is the length of the time series (s), T is the air temperature (or any scalar), t is time (s), and r is the time lag (s). Detailed descriptions of the Van Atta (1977) procedure for resolving the ramp characteristics from structure function data can be found in Van Atta (1977), Spano et al. (1997a), Chen et al. (1997a), and Shapland et al. (2012a).

2.2. Thermocouple frequency response

The response characteristics of a thermocouple are described by a first-order differential equation, because a single form of energy storage, i.e., the thermal inertia of the sensor, is dominant.

$$T_o(t) + \tau \frac{dT_o}{dt} = T_i(t) \quad (3)$$

where $T_o(t)$ is the output or the response of the system (i.e., sensor temperature), τ is the time constant (s), and $T_i(t)$ is the input function (i.e., air temperature).

2.3. Time constant

The time constant is derived from concepts of conservation and energy transfer between the sensor and the surrounding environment (McGee, 1988). Assuming the thermocouple sensor geometry is best described as a cylindrical wire,

$$\tau = \frac{\rho_w C_w d^2}{\gamma k Nu} \quad (4)$$

where ρ_w is calculated as the density of the wire, C_w is the specific heat of the wire, d is the diameter of the wire (m), $\gamma = 4$, k is the molecular thermal conductivity of air at standard temperature and pressure ($2.53 \times 10^{-2} \text{ J m}^{-1} \text{ s}^{-1} \text{ K}^{-1}$), and Nu is the Nusselt number. The Nusselt number for a cylinder (Collis and Williams, 1959) is as follows:

$$Nu = 0.24 + 0.56Re^{0.45} \quad (\text{cylinder}) \quad (5a)$$

where Re is the Reynolds number, i.e., $Re = ud/\nu$ (Reynolds, 1883), u is the mean wind speed (m s^{-1}), and ν the kinematic molecular viscosity of air at standard temperature and pressure ($1.461 \times 10^{-5} \text{ m}^2 \text{ s}^{-1}$).

The time constant calculation calls for the density and specific heat of a wire, but a thermocouple is constructed of two wires of different alloys. The physical and thermal properties at the junction of the two wires, where the air temperature influences the sensor signal, are most relevant to the time constant, but the weld of the two alloys makes these properties difficult to obtain. The densities of the wires at the junction, therefore, are approximated as the mean of the densities of the two wire types (8825 kg m^{-3} ; McGee, 1988). Similarly, the specific heats of wires at the junction are approximated as the mean of the specific heats of the two wire types ($420.49 \text{ J kg}^{-1} \text{ K}^{-1}$; McGee, 1988).

The thermocouple geometry at the junction may be spherical instead of cylindrical. In this case, ρ_w is also approximated as the mean density of the two wires, C_w is approximated as the mean specific heat of the two wires, d is the diameter of the spherical junction (m), $\gamma = 8$, and the Nusselt number according to Collis and Williams (1959) is the following:

$$Nu = 2.00 + 0.18Re^{0.67} \quad (\text{sphere}) \quad (5b)$$

Unless otherwise noted, the thermocouple geometry in this study is assumed cylindrical, and the time constants are calculated using measured wire diameters, constant values for molecular thermal conductivity and kinematic molecular viscosity, and the mean wind velocity.

2.4. Time-domain compensation

The thermocouple signal is compensated in the time domain by substituting into Eq. (3) the thermocouple temperature for $T_o(t)$, the time constant for τ , and differencing the thermocouple temperature at the shortest possible time step (i.e., the sampling interval) for approximating dT_o/dt .

2.5. Lag-domain compensation

The time-domain compensation in the surface renewal paradigm is computationally expensive because each temperature data point in the time series must be processed twice: first, to compensate the signal; and second, to calculate the structure function from the compensated signal. In the interest of developing an online processing system, it would be convenient to store only a short range of structure function values and compensate these data directly, avoiding the need to store, call, and process large amounts of time series data with more than one pass.

To derive the direct compensation of the structure function values, the right hand side of Eq. (3) is substituted for the air temperature in the structure function Eq. (2), and the terms are rearranged.

$$\overline{S^n(r)}_l = \frac{1}{L} \int_0^L \left\{ [T_o(t) - T_o(t-r)] + \tau \frac{d[T_o(t) - T_o(t-r)]}{dr} \right\}^n dt \quad (6)$$

where $\overline{S^n(r)}_l$ is the air temperature structure function, i.e., the compensated thermocouple structure function. Letting $n = 2, 3$, and 5,

the compensated thermocouple second-, third-, and fifth-order structure function are as follows:

$$\overline{S^2(r)}_i = \overline{S^2(r)}_o + 2\tau \overline{\frac{dS^1(r)_o}{dr}} + \tau^2 \overline{\left[\frac{dS^1(r)_o}{dr} \right]^2} \quad (7a)$$

$$\begin{aligned} \overline{S^3(r)}_i = \overline{S^3(r)}_o &+ 3\tau \overline{\frac{dS^2(r)_o}{dr}} + 3\tau^2 \overline{S^1(r)_o} \overline{\left[\frac{dS^1(r)_o}{dr} \right]} \\ &+ \tau^3 \overline{\left[\frac{dS^1(r)_o}{dr} \right]^3} \end{aligned} \quad (7b)$$

$$\begin{aligned} \overline{S^5(r)}_i = \overline{S^5(r)}_o &+ 5\tau \overline{S^4(r)_o} \overline{\frac{dS^1(r)_o}{dr}} + 10\tau^2 \overline{S^3(r)_o} \overline{\left[\frac{dS^1(r)_o}{dr} \right]^2} \\ &+ 10\tau^3 \overline{S^2(r)_o} \overline{\left[\frac{dS^1(r)_o}{dr} \right]^3} + 5\tau^4 \overline{S^1(r)_o} \overline{\left[\frac{dS^1(r)_o}{dr} \right]^4} \\ &+ \tau^5 \overline{\left[\frac{dS^1(r)_o}{dr} \right]^5} \end{aligned} \quad (7c)$$

The structure function of the time-domain compensated signal is equivalent to the lag-domain compensation (data not shown). The lag-domain compensation may be useful for other structure function applications, such as the cascade of isotropic turbulence from larger to smaller scales (Kolmogorov, 1941), the estimation of sensible heat flux density using Monin–Obukhov similarity theory (Wyngaard et al., 1971) or scintillometry (Coulter and Wesely, 1980), and the analysis of radar, SODAR, and LIDAR to estimate boundary-layer capping inversion characteristics (Wyngaard and Lemone, 1980; Stull, 1988).

2.6. Frequency-domain compensation

Frequency-domain compensation is convenient for eddy covariance flux estimation because transfer functions correct the cospectrum for sensor frequency response characteristics and the covariance is recovered from the integral of the cospectrum. The transfer function for compensating the spectrum can be written as

$$h(\omega) = \frac{1}{1 - i\omega\tau} \quad (8)$$

where $h(\omega)$ is the transfer function, $\omega = 2\pi f$ (f is the frequency (s^{-1})), and $i = \sqrt{-1}$.

In surface renewal signal processing, compensating the scalar signal for thermal inertia attenuation in the frequency domain offers no advantage in terms of computational expense and processing convenience because the third- and fifth-order structure functions must be calculated from the time-domain signal; only the second-order structure function is interchangeable with the Fourier transform (Monin and Yaglom, 1975). It is more direct and convenient to correct the signal in the time-domain or lag-domain rather than taking the Fourier transform, compensating the spectrum, and inverting it back into the time-domain to finally calculate the structure function. In this paper, the time-domain procedure is used to compensate the thermocouple signals. The frequency-domain and time lag domain compensation are only used to compare against the time-domain compensation.

2.7. Ramp signal to noise ratio

Because the ramp amplitude is cubed when calculating the ramp period (Van Atta, 1977), errors in the estimation of the ramp

amplitude are propagated in the ramp period term. A method for estimating the ramp signal to noise ratio (RSNR) for both Scale One and Scale Two is helpful for evaluating compensation performance and for determining the error source.

Following the assumptions of the [Van Atta \(1977\)](#) procedure, the turbulent (hence, measurable) second-order structure function is the sum of the random and coherent ramp contributions.

$$\overline{S^2(r)} = \overline{S^2(r)_c} + \overline{S^2(r)_r} \quad (9)$$

where $\overline{S^2(r)}$ is second-order structure function as calculated from the time series data, $\overline{S^2(r)_c}$ is the second-order structure function of the coherent ramp part of the signal, and $\overline{S^2(r)_r}$ is the second-order structure function of the random part of the signal.

The third-order structure function is equal to the third-order structure function of the coherent ramp signal, which for time lags much shorter than the gradual rise period is written as follows:

$$\overline{S^3(r)} = \overline{S^3(r)_c} = -\frac{a^3 r}{(d+s)} \quad (10)$$

Therefore, the second-order structure function of the coherent ramp signal for time lags much shorter than the gradual rise period is

$$\overline{S^2(r)_c} = \frac{a^2 r}{(d+s)} = -\frac{\overline{S^3(r)}}{a} \quad (11)$$

Substituting Eq. (11) into the second-order structure function Eq. (9), we arrive at the second-order structure of the noise signal as proposed by [Van Atta \(1977\)](#).

$$\overline{S^2(r)_r} = \overline{S^2(r)} + \frac{\overline{S^3(r)}}{a} \quad (12)$$

The ramp amplitude term is squared to derive a dimensionless RSNR as follows:

$$RSNR = \frac{a^2}{\overline{S^2(r)_r}} = \frac{a^2}{\overline{S^2(r)} + (\overline{S^3(r)}/a)} \quad (13)$$

For a two-scale ramp model, a similar procedure can be followed in conjunction with the assumptions and derivations from [Shapland et al. \(2012a\)](#) to arrive at an equation for the RSNR for Scale One (the smaller scale) and Scale Two, although the stepwise details of the derivation are omitted here for the sake of brevity. The RSNR for a one-scale ramp model and the RSNR for Scale One of a two-scale ramp model are nearly equivalent.

$$RSNR \cong RSNR_1 \quad (14a)$$

where $RSNR_1$ is the Scale One RSNR. The time lag is increased so that the second- and third-order structure functions of the ramp signal represent only the larger ramp scale, the Scale Two ramp amplitude is resolved, and the structure function and ramp amplitude are used to determine the Scale Two RSNR.

$$RSNR_2 = \frac{a_2^2}{\overline{S^2(r)_r}} = \frac{a_2^2}{\overline{S^2(r)} + (\overline{S^3(r)}/a_2)} \quad (14b)$$

where $RSNR_2$ is the Scale Two RSNR.

3. Materials and methods

3.1. Site and instrumentation

Data were collected over a bare soil field from September 16, 2010 to September 24, 2010 and a sorghum (*Sorghum bicolor*) field from July 22, 2010 to July 30, 2010. Both fields were located on the Campbell Tract (38°32' N, 121°46' W) at the University of California, Davis, CA, U.S.A. Fetch in the prevailing wind direction (South) was

200 m for the bare soil field and 100 m for the sorghum field, and the sorghum canopy was 0.6 m tall.

Tri-axial sonic anemometers (CSAT3, Campbell Scientific Inc., Logan, UT, U.S.A.) were installed at 1 m over the bare soil and at 1.4 m above ground over the sorghum canopy. At the bare soil and sorghum field sites, there were three sets of three cross-welded type E thermocouples. Each thermocouple set had a different nominal wire diameter: 13, 25, or 76 μm diameter wire (FW05, FW1, FW3, respectively, Campbell Scientific Inc., Logan, UT, U.S.A.). The exposed thermocouple junctions were positioned in a row 0.1 m posterior and 0.05–0.15 m lateral to the anemometer sampling volume relative to the prevailing wind. Each experimental site had one row of exposed thermocouple junctions that was approximately 0.1 m in length and ran laterally away from the anemometer sampling volume. Each thermocouple junction in the row was about 0.01–0.02 m laterally from the adjacent thermocouple junction. All sensors were sampled at 20 Hz.

Prior to deployment in the field, the thermocouple wire and junction diameters were measured. A stage micrometer (Micro-master Microscope Stage Micrometer, Fisher Scientific Company LLC, Pittsburgh, PA, U.S.A.) was used to calibrate a light microscope (Micromaster Microscope, Fisher Scientific Company LLC, Pittsburgh, PA, U.S.A.), and an image of the stage micrometer was taken using a digital camera (Leica Microsystems Inc., Buffalo Grove, IL, U.S.A.). Each thermocouple was placed under the microscope, a photograph was taken, and the scale from the stage micrometer was used to measure both the wire diameter and the thermocouple junction at three cross-sections. The wire and junction diameters were calculated from the mean of the three measurements. The nominal 13 μm diameter thermocouples had measured wire diameters of 16, 14, and 14 μm and 13, 13, and 13 μm for the bare soil and sorghum sites, respectively. The nominal 25 μm diameter thermocouples had measured wire diameters of 29, 27, and 27 μm and 27, 25, and 25 μm for the bare soil and sorghum sites, respectively. The nominal 76 μm diameter thermocouples had measured wire diameters of 83, 81, and 86 μm and 92, 84, and 79 μm for the bare soil and sorghum sites, respectively. The thermocouples are hereafter referred to by their nominal wire diameter, e.g., the 13 μm thermocouple.

3.2. Surface renewal processing scheme

The second-, third-, and fifth-order structure function were calculated for each thermocouple over the 30 min sampling interval. The structure function time lag was set to the time lag associated with the microfront duration (r_m), as described in [Chen et al. \(1997a\)](#), and the [Van Atta \(1977\)](#) procedure was used to resolve the Scale One (smaller scale) ramp amplitude, a_1 (K), and ramp period, $(d+s)_1$ (s) (see Fig. 1). The Scale Two (larger scale) ramp amplitude, a_2 (K), and ramp period, $(d+s)_2$ (s), were resolved by setting the structure function time lag to either the Scale One gradual rise period, d_1 (s), or one half of the Scale One ramp period, $(d+s)_1/2$, depending on the smaller-scale ramp intermittency (see [Shapland et al., 2012a](#) for more details). The mean of each ramp characteristic resolved from the three thermocouples of a given size was compared against the mean of the same ramp characteristic resolved from the three thermocouples of another size. This process was repeated for each ramp characteristic: the Scale One ramp amplitude, a_1 , the Scale One ramp period, $(d+s)_1$, the Scale Two ramp amplitude, a_2 , and the Scale Two ramp period, $(d+s)_2$.

The surface renewal flux for Scale One is calculated using the Scale One ramp characteristics.

$$H_{SR_1} = \alpha_1 z \rho C_p \frac{a_1}{(d+s)_1} \quad (15)$$

Table 1

Site, instrumentation, and processing parameters for the studies included in the meta-analysis. In some studies, the time lag was set to r_m , the time lag at which occurs the maximum absolute value of the third-order structure function divided by the time lag.

Author	Surface	Canopy height	Measurement height	Thermocouple diameter	Time lag
Snyder et al. (1996)	Grass	0.1	0.3, 0.6, 0.9, 1.2	76	0.25, 0.5, 0.75, 1.0
Spano et al. (1997a)	Wheat	0.7	0.7, 1.0, 1.3	76	0.25, 0.5, 0.75, 1.0
Spano et al. (1997a)	Sorghum	0.7	0.7, 1.0, 1.3	76	0.25, 0.5, 0.75, 1.0
Spano et al. (1997b)	Vineyard	2.0	2.0, 2.3, 2.6, 2.9	76	0.25, 0.5
Spano et al. (1997b)	Avocado orchard	5.2	5.2, 5.8, 6.1	76	0.25, 0.5
Spano et al. (2000)	Vineyard	2.1	2.1, 2.4, 2.7	76	0.25, 0.5
Spano et al. (2000)	Vineyard	2.2	2.2	76	0.25, 0.5
Zapata and Martinez-Cob (2001)	Lagoon	0.0	0.9, 1.1, 1.4	76	0.25, 0.375, 0.5, 0.75
Snyder et al. (2006)	Grassland	0.25	1.0	76	0.25, 0.5
Snyder et al. (1997)	Citrus orchard	4.2	4.5	76	0.5, 1.0
Moratiel and Martinez-Cob (2011)	Rice	0.05, 0.16, 0.44, 0.68	0.3, 0.6, 0.7, 0.8, 0.9, 1.0, 1.4, 1.45, 1.55, 1.7	76	0.75
Shapland et al. (2012b)	Bare soil	0.0	0.5, 1.0, 1.5, 2.0	13	r_m
Shapland et al. (2012b)	Sorghum	0.8	1.4	13, 25	r_m
Shapland et al. (2012c)	Vineyard	2	2.13	76	0.25, 0.5
Shapland et al. (2012d)	Wheat	0.9	1.35	76	0.5

where H_{SR_1} is the Scale One surface renewal sensible heat flux (W m^{-2}), α_1 is the alpha calibration for Scale One, z is the measurement height (m), ρ is the density of air (kg m^{-3}), and C_p is the specific heat of air ($\text{J K}^{-1} \text{kg}^{-1}$). The surface renewal flux for Scale Two is calculated using the Scale Two ramp characteristics.

$$H_{SR_2} = \alpha_2 z \rho C_p \frac{a_2}{(d+s)_2} \quad (16)$$

where H_{SR_2} is the Scale Two surface renewal sensible heat flux (W m^{-2}) and α_2 is the alpha calibration for Scale Two.

Data were not accepted: (1) if the Scale One (smaller scale) gradual rise period was longer than the Scale One ramp period; (2) if the Scale One ramp period was longer than the Scale Two (larger scale) ramp period; (3) if the absolute value of the Scale One ramp amplitude was less than 0.05 K; and (4) in the few near-neutral stability cases when the Scale Two ramp periods were orders of magnitude longer than the length of the time series. Data were sorted by stability according to the sign of the air temperature third-order structure function (Van Atta, 1977).

3.3. Eddy covariance processing scheme

A 2-dimensional coordinate rotation was performed on each 30 min interval of sonic anemometer data. For each thermocouple regardless of wire diameter and relative position with respect to the other thermocouples, the lag between the vertical wind speed and the thermocouple signal was removed by maximizing the correlation coefficient prior to the eddy covariance calculations. The thermocouple air temperature measurements (and not the sonic temperature) were used as the scalar in the eddy covariance sensible heat flux density calculation unless otherwise noted. Analysis was performed only on data intervals with a mean wind direction within 45° of the prevailing wind direction (the anemometer direction), for which the momentum flux density was less than zero, and with a horizontal wind speed greater than 0.05 m s^{-1} .

At both experimental sites, the sonic anemometer was relatively close to the underlying surfaces, so eddies that contributed the most to the flux may have been large relative to the path length of the sonic anemometer. Therefore, spatial averaging over the sonic anemometer path length may have resulted in an underestimation of the flux from the smaller eddies. Using EddyPro (LI-COR, Inc., Lincoln, NE, U.S.A.), sensible heat flux density estimations without a correction for spatial averaging along the horizontal, crosswind or vertical components were compared against sensible heat flux estimations with the correction. The sensible heat flux estimations with the correction were 5% greater over both the bare soil and the sorghum. The relatively small differences signify that there

was not gross flux underestimation due to the sensor installation heights. Except for the EddyPro analysis of path length averaging, data processing, analysis, and graphics generation were performed with R Statistical Software (R Development Core Team, 2012) using scripts written by the authors.

4. Meta-analysis procedures

The surface renewal literature was searched for reported alpha calibrations used in sensible heat flux density measurements from thermocouple signals. Only studies that relied on the Van Atta (1977) procedure to resolve the temperature ramps were used in the meta-analysis to eliminate uncertainties associated with discrepancies in ramp resolution methods. Alpha calibrations based on the combined surface renewal and similarity theory approach (Castellvi, 2004) were omitted because the transfer coefficients used in this scheme were derived for longer time scales (Stull, 1988) than those associated with coherent structures (e.g., Paw U et al., 1992) and therefore are not valid for describing transfer within the coherent structures. Studies that did not report the alpha calibration or its coefficient of determination, the thermocouple size, and the sensor height were omitted from the meta-analysis. If the averaging interval for the structure function and eddy covariance were not the same, then the alpha calibrations were discarded. The thermocouple had to be located at the canopy top or higher for inclusion of the corresponding alpha calibration in the meta-analysis. A low coefficient of determination in the alpha calibration regression analysis indicates poor slope estimation and hence a compromised estimation of the alpha calibration. Alpha calibrations in the literature with coefficients of determination less than 0.6 were therefore omitted. This value was chosen as a compromise between culling so many data points that the meta-analysis is weakened and keeping too many data points of questionable fidelity. The 77 alpha calibrations from 11 articles that met these criteria include a broad range of surface architecture, canopy heights, thermocouple heights, and structure function time lags (Table 1). Because the conventional Van Atta (1977) procedure identifies the smaller scale ramps (Scale One), the alpha calibrations from these studies are the Scale One alpha calibration. The majority of this paper therefore focuses on Scale One, allowing for the correction of the alpha calibrations in the literature for thermocouple frequency response effects, even though Shapland et al. (2012b) showed that Scale Two is responsible for the flux.

Separate alpha calibrations for unstable and stable thermal stratification regimes are infrequently reported, so all the data regardless of the stability were used in deriving the coefficient to correct the reported alpha calibrations in the literature for

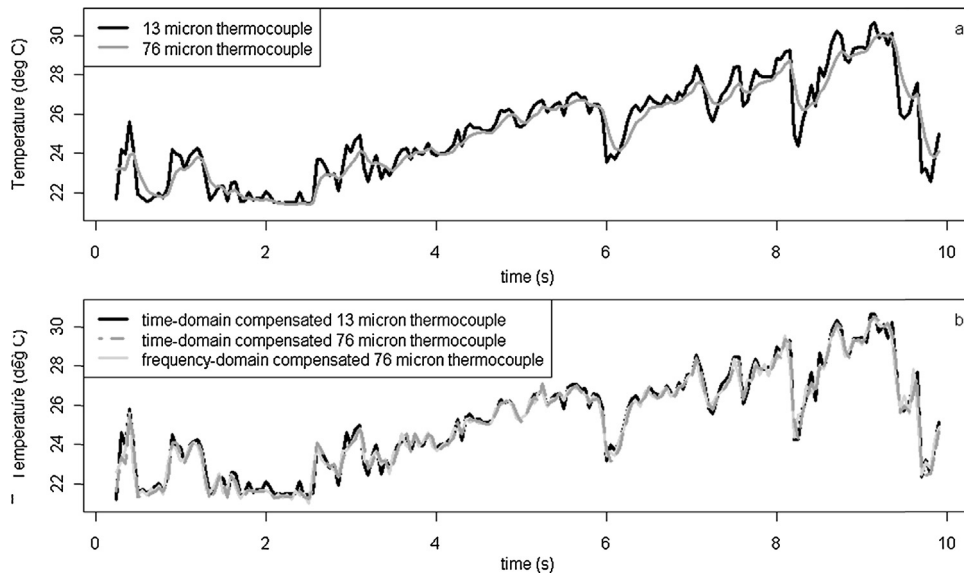


Fig. 2. Time series of (a) air temperature from 13 and 76 μm diameter thermocouples, and (b) time- or frequency-domain compensated 13 and 76 μm diameter thermocouples.

frequency response characteristics. In the few cases where the alpha calibrations were reported by stability, only the unstable alpha calibration is used in the meta-analysis because the absolute value of the heat fluxes for unstable conditions were assumed greater compared to those from stable conditions and therefore more strongly influenced the alpha calibration regression analysis. No attempt was made to account for frequency response characteristics on eddy covariance estimations because the eddy covariance temperature scalar (i.e., air temperature or sonic temperature) was not always clearly defined in the individual studies and the sensor frequency response influences eddy covariance minimally compared to its influence on surface renewal.

To justify our approach to the meta-analysis and these data quality control procedures, we establish: (1) that the sensor frequency response attenuates the Scale One (i.e., conventional) surface renewal flux estimation (Sections 5.1 and 5.2); (2) that the Scale One surface renewal flux estimation decreases with increasing sensor diameter and response time (Section 5.2); (3) that the relationship between the Scale One surface renewal flux estimations using raw and compensated thermocouple signals is linear (Section 5.2); (4) that the compensation procedures described in this paper correct for the effects of frequency response with sufficient accuracy (Sections 5.2 and 5.3); and (5) that the errors associated with frequency response compensation are much less influential for eddy covariance flux estimation compared to Scale One surface renewal flux estimation (Section 5.3).

Once the meta-analysis has been performed (Section 5.4), then the effect of the compensation procedure on the Scale Two surface renewal flux estimation is examined (Section 5.5), and the sources of errors in the compensation procedure are addressed (Sections 5.6 and 5.7).

5. Results and discussion

5.1. Time series of raw and compensated thermocouple signals

The 76 μm thermocouple does not respond as rapidly to temperature fluctuations as the 13 μm thermocouple, so the signal from the larger sensor appears smoother in the time series trace (Fig. 2a). The thermal inertia of the sensor acts as a low-pass filter (McGee, 1988), dampening the apparently random air temperature fluctuations superimposed on the ramps. Ramp amplitudes from the

76 μm thermocouple are attenuated relative to those from the 13 μm thermocouple signal and occur over a longer period of time, prolonging the apparent microfront duration (e.g., the ramp amplitudes at approximately 6, 8, and 9.5 seconds in Fig. 2a). The time- and frequency-domain compensated 76 μm sensor signals align closely with one another and with the time-domain compensated 13 μm thermocouple signal, tracking the random fluctuations, the microfront durations, and the ramp amplitudes (Fig. 2b). Because the frequency response characteristics of the 13 μm thermocouple more or less include the highest appreciable air temperature fluctuations, the differences between the raw and compensated 13 μm thermocouple signals are minimal (Fig. 2a and b). The data presented in Fig. 2a and b were collected over the bare soil at one meter height from September 21, 2010 from 12:00 to 12:30 during unstable conditions, and raw and compensated temperature traces from varying thermal stability regimes over both the bare soil and the sorghum have similar relationships (data not shown).

The time- and lag-domain compensated signals are equivalent, but they differ slightly from the frequency-domain compensated signals. Even though all three compensation procedures should theoretically produce the same results, the particulars of the Fourier transform can produce a compensated signal that is slightly different from the time-domain (Bloomfield, 2000), and therefore lag-domain, compensated signals. The discrepancies between the compensated signals are minimal (Fig. 2a and b), so the choice of domain for the compensation depends on which is most convenient for a given application. In the case for this paper, the time-domain compensation was performed on the data collected in the bare soil and sorghum experiments, because it was both convenient for processing stored data sets and equivalent to the lag-domain compensation, which is convenient for online processing.

5.2. Scale One surface renewal from raw and compensated thermocouple signals

The ratio of the ramp amplitude to the ramp period is important in surface renewal flux estimation (Paw U et al., 1995; see Eqs. (15) and (16)). For time lags less than r_m the Van Atta (1977) procedure attenuates the ratio of the ramp amplitude to ramp period for Scale One (Shapland et al., 2012a), and r_m increases with measurement height and canopy height (Chen et al., 1997a,b). Consistent with the prolonged microfront durations observed in the larger

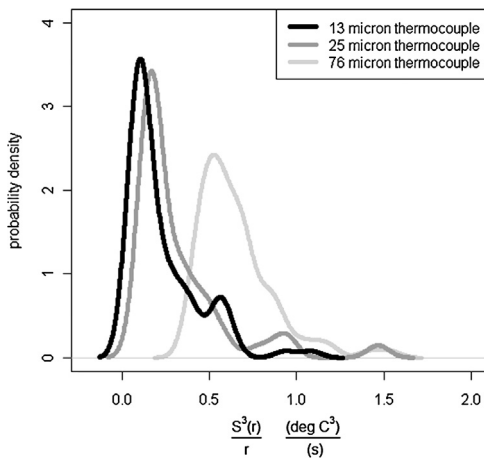


Fig. 3. Probability density of the third-order structure function divided by the time lag plotted against the time lag from the 13, 25, and 76 μm diameter thermocouples for the bare soil experiment during unstable conditions.

diameter thermocouple signal (Fig. 2a), r_m also increases with thermocouple size (Fig. 3). For online measurement systems, a longer range of structure function time lags therefore must be calculated and stored in a data logger if the more robust thermocouples are deployed. Alternatively, direct compensation of the structure function values reduces the range of required time lags. Although only data from the bare soil experiment during unstable conditions were included in Fig. 3 for the sake of clarity, the relationships for r_m among the three thermocouple sizes are the same for both unstable and stable conditions at both sites (data not shown).

Once the appropriate r_m has been determined, the structure function values are passed into the Van Atta (1977) procedure to determine the ratio of the ramp amplitude to the ramp period. The ratio of the ramp amplitude to the ramp period from the raw 25 μm thermocouples underestimates the ratio from the raw 13 μm thermocouples (Table 2). The mean of the regression slopes from the bare soil and sorghum surfaces is 1.18, and the coefficients of determination are high. When the 13 μm and 25 μm thermocouple signals have been compensated, the mean of the regression slopes is 1.02 (Table 2). Because the compensation procedure produces accurate results for the 25 μm thermocouple and the thermocouples of this size are only modestly more rugged than the 13 μm sensors, further evaluation of the compensation for the 25 μm thermocouple is omitted throughout this paper for the sake of brevity.

The raw 76 μm thermocouple signal also underestimates the ratio of the ramp characteristics compared to the same ratio from the raw 13 μm thermocouple signal (Table 2 and Fig. 4). The underestimation is consistent with the observation of attenuated ramp

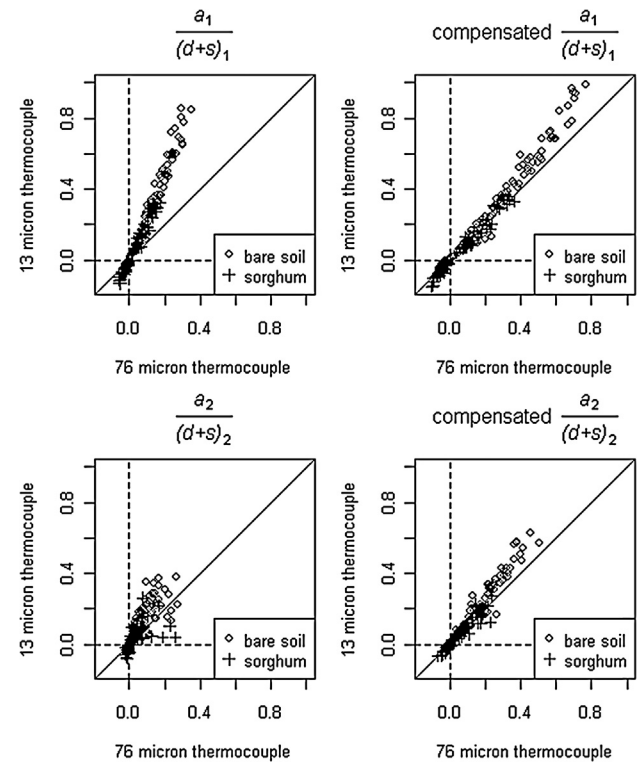


Fig. 4. Regression plots for estimated ratio of the ramp amplitude to ramp period, as measured using the 13 μm diameter thermocouple, against the same ratio measured with the 76 μm diameter thermocouple. The subscripts 1 and 2 correspond to Scale One (the smaller embedded scale) and Scale Two (the larger scale), respectively.

amplitudes from the raw 76 μm sensor in Fig. 1., the ratio of the ramp characteristics from the raw 13 μm thermocouple sensor are 2.38 and 1.93 times the ratios from the raw 76 μm thermocouple (Table 2 and Fig. 4) for the bare soil and sorghum, respectively. The coefficients of determination are high, indicating that the ratio of the ramp characteristics from each sensor size is linearly related to each other. Therefore, the ratio from the 13 μm diameter sensor can be estimated by applying the regression slope coefficient to the ratio from the 76 μm diameter sensor. Using data collected over bare soil and the Van Atta (1977) procedure (i.e., Scale One ramp characteristics), Duce et al. (1997) also reported a decrease in the estimated surface renewal sensible heat flux, and hence a decrease in the ratio of the ramp amplitude to ramp period, with increasing thermocouple diameter.

When the signals from the 76 μm and 13 μm thermocouple are compensated, the ratios from each sensor more closely agree with one another (Table 2 and Fig. 4). The mean of the two regression slopes from the bare soil and sorghum surfaces is 1.12. This is within the expected range of error for micrometeorological measurements such as eddy covariance (e.g., Massman and Lee, 2002; Mauder et al., 2007; Kochendorfer et al., 2012). For both surfaces, the compensated 76 μm thermocouple tends to slightly underestimate the ratio and the coefficients of determination are greater than 0.90.

The time constant used in the compensation procedure is a function of the thermocouple geometry, so it is of interest to compare results using time constants based on the nominal wire diameter, the measured wire diameter, and the measured wire junction to determine the most appropriate sensor dimension for the time constant calculation. If the nominal wire diameter is used instead of the measured wire diameter, the regression slopes and coefficients of determination are almost always further from unity (Table 2). Other approaches to calculating the time constant, such as using the measured thermocouple junction diameter and

Table 2

Regression coefficients for estimated Scale One (the smaller embedded scale) ratio of the ramp amplitude to ramp period, as measured using the 13 μm diameter thermocouple, against the same ratio measured with the 25 μm diameter thermocouple and the 76 μm diameter thermocouple. The slope of the regression analysis is indicated by ' m '. The asterisk indicates that the time constants were calculated using the nominal, rather than measured, wire diameters.

$a_1/(d+s)_1$							
Diameter (μm)	Surface	25		76			
		Signals	m	R^2	Signals	m	R^2
Bare soil	Raw		1.17	1.00		2.38	0.99
Sorghum	Raw		1.19	1.00		1.93	0.98
Bare soil	Compensated		1.00	1.00		1.19	0.97
Sorghum	Compensated		1.02	0.99		1.05	0.98
Bare soil	Compensated*		1.00	1.00		1.28	0.99
Sorghum	Compensated*		1.04	0.99		1.17	0.98

Table 3

Regression coefficients for eddy covariance as measured with the 13 μm diameter thermocouple against eddy covariance measured with the 76 μm diameter thermocouple. The slope of the regression analysis is indicated by 'm'.

Surface	Signals	<i>m</i>	R^2
Bare soil	Raw	1.11	1.00
Sorghum	Raw	1.12	1.00
Bare soil	Compensated	1.00	1.00
Sorghum	Compensated	0.98	1.00

the Nusselt number for a sphere (not shown) and instantaneous time constants based on fluctuating wind speed (not shown), also produce inferior results. It is therefore recommended that time constants are based on measured wire diameters, constant values for molecular thermal conductivity and kinematic molecular viscosity, and the mean wind velocity.

5.3. Eddy covariance from raw and compensated thermocouple signals

The frequency response characteristics of the raw 76 μm thermocouple do not affect the eddy covariance data (Table 3) as much as the ratio of the ramp amplitude to ramp period for surface renewal (Table 2). The eddy covariance calculation with the raw 76 μm thermocouple differs by an average of 12% from the eddy covariance calculation with the raw 13 μm thermocouple, and the coefficients of determination are perfect (Table 3). For surface-layer energy and mass transport, relatively low frequency spectral coefficients contribute to the majority of the total flux, while high frequency spectral coefficients contribute marginally (Monin and Obukhov, 1954). As a result, high frequency attenuation does not dramatically reduce the total flux measured via eddy covariance unless the sensors are located so close to short-canopy surfaces that the very high frequency portion of the spectrum, coinciding with the frequency range of signal attenuation, is responsible for the flux (McBean, 1972). In the surface renewal paradigm, relatively large eddies are also responsible for the majority of the flux, however, the terminus of the temperature ramp, i.e., the sudden rise or fall portion of the ramp signal that determines the ramp amplitude regardless of scale, corresponds to the high-frequency signal components that are affected by the thermal inertia of the sensors. Thus, high-frequency attenuation of the scalar (temperature) signal has a greater impact on surface renewal estimation than eddy covariance estimation.

Another consequence of the higher frequency components being less important for estimating the eddy covariance flux compared to surface renewal is that errors associated with thermocouple frequency response compensation are not as deleterious to the eddy covariance flux estimates (Table 3). The regression statistics from the compensated 76 μm thermocouple eddy covariance estimates are closer to unity than those from the raw 76 μm thermocouple eddy covariance estimates (Table 3). Some uncertainty is expected in frequency response corrections for eddy covariance (Massman and Clement, 2004), and the compensated eddy covariance estimates differ by only about 2% (Table 3), which is well within the range of expected error for eddy covariance flux estimates (e.g., Massman and Lee, 2002; Mauder et al., 2007; Kochendorfer et al., 2012). The accuracy of the compensated eddy covariance data shows that the time constant calculation and compensation procedures used in this paper are sufficient and solar loading has a negligible effect, so the errors in the surface renewal compensation must stem from another source, such as the particulars of ramp resolution and surface renewal signal processing. This will be investigated further in Sections 5.6 and 5.7.

5.4. The alpha calibration

The alpha calibration values for the bare soil and sorghum experiments using the raw and compensated thermocouple signals are listed in Table 4. For data that have not been screened for stability conditions, the raw thermocouple signals yield alpha calibrations ranging from 0.32 to 0.88. The alpha calibrations from the compensated signals span a smaller range from 0.28 to 0.38. The frequency response characteristics of the thermocouple apparently have a greater influence on the alpha calibration compared to the differences in surface architecture and measurement height between the bare soil and sorghum experiments. Assuming that the air parcels are uniformly heated or cooled at the bare soil site because there was no plant canopy to induce vertically heterogeneous energy exchange (Paw U et al., 1995), the convergence of the alpha calibration at both the bare soil and sorghum sites suggests that other physical processes cause its departure from unity, such as effective air parcel dimensions (Spano et al., 1997a), micro-advection processes within the coherent structure (Paw U et al., 1995, 2005), or embedded scales (Shapland et al., 2012b).

The coefficients of determination in the alpha calibrations from the 13 and 25 μm diameter raw thermocouple signals are only marginally lower than those from the 76 μm diameter raw thermocouple signals (Table 4). Furthermore, the coefficients of determination from the compensated thermocouple signals of all sizes are equal or marginally higher than those from the raw thermocouple signals (Table 4). Thus, neither the 13 or 25 μm diameter sensors nor compensated 76 μm diameter sensors compromise the precision of surface renewal sensible heat flux measurements. Duce et al. (1997), however, obtained higher coefficients of determination in the alpha calibration regression from raw 76 μm diameter thermocouples compared to raw 13 μm diameter thermocouples, but their results are less reliable because the coefficients of determination were less than 0.6 even for the largest thermocouple. The alpha calibration values for the unstable data set (Table 4) are similar to those for the data that have not been separated by stability, but the calibration was less for the stable data set. Lower alpha calibrations for stable data sets have been reported in other surface renewal studies such as Paw U et al. (1995), but that study did not use structure function analysis. For the stable data in the bare soil experiment, the coefficients of determination for the alpha calibration are so low that they do not meet the minimum coefficient of determination criterium for the meta-analysis. This is likely due to the small range of negative heat flux density values at this site, coupled with errors in the eddy covariance data associated with low turbulence conditions (Fig. 4).

A meta-analysis of surface renewal studies over other surface types and measurement heights is useful to test whether the convergence of the alpha calibration values at the bare soil and sorghum site was coincidental. Since it has been established here that the frequency response characteristics cause 76 μm and 25 μm diameter thermocouples to underestimate the ratio of the ramp amplitude to ramp period linearly, it is possible to correct the reported alpha calibrations in the surface renewal literature. The reported alpha calibrations from studies using 76 μm diameter thermocouples were divided by the slope coefficient, 2.16, from the regression analysis for the raw 13 μm thermocouple data against the raw 76 μm thermocouple data. For the study that used a 25 μm diameter thermocouple, the reported alpha calibration was divided by the corresponding regression slope coefficient, 1.18.

The reported alpha calibrations in the literature converge once they have been corrected for thermocouple frequency response characteristics (Fig. 5a). The uncorrected alpha calibrations have a mean value of 0.83 and a standard deviation of 0.33, whereas the corrected alpha calibrations have a mean value 0.41 and standard deviation 0.14. Assuming the distributions of calibration values are

Table 4

Regression coefficients for the eddy covariance sensible heat flux and the Scale One (the smaller scale) surface renewal sensible heat flux. Alpha is the slope of the regression.

Stability	Surface	Signals	Diameter (μm)	Unstable		Stable		All	
				Alpha	R^2	Alpha	R^2	Alpha	R^2
Bare soil	Raw	13	0.36	0.94	0.12	0.57	0.36	0.94	
			25	0.43	0.94	0.14	0.57	0.43	0.94
			76	0.88	0.95	0.26	0.54	0.88	0.95
Sorghum	Raw	13	0.36	0.96	0.21	0.96	0.32	0.91	
			25	0.43	0.97	0.27	0.95	0.38	0.92
			76	0.70	0.98	0.43	0.91	0.63	0.93
Bare soil	Compensated	13	0.31	0.94	0.10	0.53	0.31	0.94	
			25	0.31	0.94	0.09	0.52	0.31	0.94
			76	0.38	0.95	0.07	0.48	0.38	0.94
Sorghum	Compensated	13	0.31	0.96	0.20	0.96	0.28	0.93	
			25	0.32	0.97	0.23	0.93	0.29	0.94
			76	0.32	0.98	0.24	0.94	0.31	0.96

normal, 95% of the uncorrected alpha values are within the range of 1.17–0.51, while 95% of the corrected alpha values are within the range of 0.55–0.27. The mean and variability of the uncorrected and corrected alpha calibrations are similar to those observed in the bare soil and sorghum experiments, so the findings from those two experiments were not coincidental. Although variations in site, installation, and turbulence may also affect the alpha calibration, as previously hypothesized, it is clear from Fig. 5a that the frequency response characteristics of the thermocouple are the prevailing influence on the alpha calibrations reported in the literature.

The mean value from the corrected alpha calibrations is similar to the value predicted by Paw U et al. (1995) to account for uneven heating of the air parcel. It is also similar to the relative size of the smaller, embedded scale (Scale One) to the larger, flux-bearing scale (see Fig. 7a and b in Shapland et al., 2012b), which also led to an alpha calibration of about 0.5 for conventional Scale One surface renewal flux. The compensation procedure and meta-analysis provide an alpha calibration for obtaining more accurate sensible heat flux measurements via surface renewal than were previously possible without calibration against eddy covariance, but it is important to emphasize that the alpha calibration from the meta-analysis is empirical in nature. It does not provide an explanation of the theoretical underpinnings of the alpha calibration. More work is needed to reconcile the various existing theories about the physics of the alpha calibration, and in these future studies the frequency response characteristics of the sensor must be compensated.

Similar to observations from individual surface renewal studies in the literature, the corrected alpha calibrations in the meta-analysis decrease linearly with height (Fig. 5b). It may therefore be possible to obtain even closer empirical alpha calibrations by correcting for the measurement height using the line fit to the linear

decrease in the alpha calibration. The decrease in the alpha calibration with measurement height may be due to the same reasons as suggested in the individual surface renewal studies that observed the same phenomenon, such as the sensor placement relative to the coherent structure height (Spano et al., 1997a). Also, a fixed structure function time lag, rather than r_m , was used in most of the studies. The r_m parameter increases with taller canopies (Chen et al., 1997a,b) and therefore higher measurement heights, so the high-frequency signal attenuation may not affect ramp signals as much from taller canopies compared to smaller canopies. Both the linear decrease with height and the scatter about the fitted line may also be a vestige of correcting the reported alpha calibrations by a constant value for each sensor size, rather than compensating the thermocouple signals with measured time constants, which is impossible without access to the raw turbulence data from the experiments reported in the literature.

The variability in the corrected alpha calibrations also may be the result of the site-specific conditions and experimental design that influence the physical processes of the alpha calibration, as well as the mismatch of scalars used in surface renewal and eddy covariance (i.e., air temperature and sonic temperature) and the tendency in the literature to report only one alpha calibration for all stability regimes (e.g., Spano et al., 1997a,b; Snyder et al., 2006). Flux density calculations based on the sonic temperature approximate the buoyancy flux, but calculations based on air temperature yield the sensible heat flux. For measurements over surfaces with high rates of latent heat flux density, the buoyancy flux is somewhat greater than the sensible heat flux. Under these conditions, if the sonic temperature was used in the eddy covariance estimates but the air temperature was used in the surface renewal estimates, then the alpha calibration would be overestimated. Furthermore, in the few studies that have reported alpha calibrations by stability regime, the stable alpha calibration is generally less than the unstable alpha calibration. There is uncertainty in the reported alpha calibrations if they are not separated by stability, and therefore the corrected alpha calibrations in the meta-analysis are affected by the same uncertainty. Also, errors in the eddy covariance measurements and varying approaches to eddy covariance post-processing corrections by individual investigators may have contributed to the variability in the meta-analysis. Due to these potential sources of variability in the reported alpha calibrations, it may be possible to refine the empirical alpha calibration by performing an analysis of turbulence data from multiple sites, ensuring the time lag parameter is set to r_m , the same scalar for eddy covariance is used for surface renewal, a uniform approach to the eddy covariance post-processing procedures are applied, and the alpha calibration is computed separately for unstable and stable conditions.

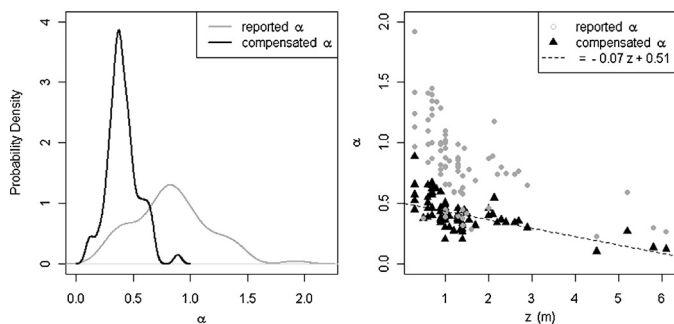


Fig. 5. (a) Probability density of the reported alpha calibrations reported in the literature and the alpha calibrations corrected for thermocouple frequency response characteristics, and (b) the reported and corrected alpha calibrations plotted against measurement height.

Table 5

Regression coefficients for estimated Scale Two (the larger scale) ratio of the ramp amplitude to ramp period, as measured using the 13 µm diameter thermocouple, against the same ratio measured with the 25 µm diameter thermocouple and the 76 µm diameter thermocouple. The slope of the regression analysis is indicated by 'm'. The asterisk indicates that the time constants were calculated using the nominal, rather than measured, wire diameters.

$a_2/(d+s)_2$					
Diameter (µm)		25		76	
Surface	Signals	m	R^2	m	R^2
Bare soil	Raw	1.08	0.97	1.39	0.80
Sorghum	Raw	1.07	0.80	0.86	0.48
Bare soil	Compensated	1.14	0.98	1.17	0.90
Sorghum	Compensated	0.96	0.89	0.92	0.87
Bare soil	Compensated*	1.07	0.94	1.35	0.96
Sorghum	Compensated*	1.00	0.90	1.09	0.84

5.5. Scale Two surface renewal from raw and compensated thermocouple signals

Scale Two has been shown to account for the surface renewal sensible heat flux over bare soil and short canopies under unstable conditions (Shapland et al., 2012b), and more work is needed to determine if Scale Two is the flux-bearing scale for taller canopies and under all stability regimes. In future investigations into surface renewal theory, it would be convenient to use the robust 76 µm diameter thermocouples rather than the more fragile sensors, so it is important to investigate the compensation procedure for Scale Two ramp resolution. In comparing the ratio of the ramp amplitude to the ramp period for the larger scale, Scale Two, from the raw 76 µm thermocouple and the raw 13 µm thermocouples, the mean of the two regression slopes from the two surfaces is 1.13 (Table 5). The coefficients of determination for Scale Two (Table 5) are relatively low compared to those from Scale One (Table 2), implying that the frequency response characteristics of the 76 µm thermocouple signal interfere with the procedure for determining the Scale Two ramp characteristics.

When the signals from the thermocouples are compensated, the Scale Two ratios from each sensor tend to more closely agree with one another (Table 5 and Fig. 4). For the compensated 76 µm diameter thermocouple signal, the mean of the regression slopes from the bare soil and sorghum surfaces for Scale Two is 1.05. This is within the expected range of error for micrometeorological measurements such as eddy covariance (e.g., Massman and Lee, 2002; Mauder et al., 2007). The coefficients of determination are greater than 0.85 for both thermocouple sizes (Table 5), representing a marked improvement compared to the ratio from the raw signals. Thus, the compensation procedure reduces the interference in resolving the Scale Two ramp characteristics from the raw 76 µm sensor due to signal attenuation.

5.6. Compensation exaggerates signal noise

Given the similar appearance of the compensated signals from both sensor sizes in the time domain (Fig. 2b), it is surprising that the regression statistics for the ratio of ramp amplitude to ramp period for Scale One (Table 2) and Scale Two (Table 5) are not closer to unity. For nearly every surface type and scale (Scale One and Scale Two), the ramp amplitude from the compensated 76 µm sensor is overestimated compared to the ramp amplitude from the 13 µm diameter sensor (Table 6), and the overestimation is to be worse for the ramp period (Table 6). The coefficients of determination from the ramp amplitude regressions are better than the coefficients of determination from the ramp period regressions regardless of scale. In the Van Atta (1977) procedure, the estimated ramp amplitude is cubed to determine the ramp period, so any

Table 6

Regression coefficients for estimated ramp amplitude and ramp period for Scale One and Scale Two, as measured using the compensated 13 µm diameter thermocouple, against the same terms measured with the compensated 76 µm diameter thermocouple. The slope of the regression analysis is indicated by 'm'. The subscripts 1 and 2 correspond to Scale One (the smaller scale) and Scale Two (the larger scale), respectively.

Surface	a_1		a_2		$(d+s)_1$		$(d+s)_2$	
	m	R^2	m	R^2	m	R^2	m	R^2
Bare soil	0.94	0.98	0.97	0.99	0.82	0.85	0.74	0.81
Sorghum	0.90	0.99	1.02	0.96	0.87	0.92	0.84	0.73

error in the ramp amplitude is propagated in the ramp period. As a result, the ratio of the ramp amplitude to the ramp period is underestimated. The propagation of error applies to the estimation of both the smaller scale (Scale One) and the larger scale (Scale Two), because both scales are resolved with a similar procedure (Shapland et al., 2012a,b).

The median RSNR is greater for the compensated 13 µm diameter sensor than for the compensated 76 µm diameter sensor for each surface, stability, and ramp scale (Table 7). Ramp formation, and hence RSNR, depends on the site characteristics, such as canopy height, shear, and measurement height (Paw U et al., 1992). For a given RSNR, the compensation procedure produces more noise in the compensated 76 µm thermocouple compared to the compensated 13 µm thermocouple. Thus, while the compensation procedure presented in this paper is broadly applicable, its accuracy depends on the aspects of the site that influence coherent structure and ramp development.

5.7. Ramp signal to noise ratio by stability and scale

For unstable conditions, the bare soil has a lower RSNR₁ and RSNR₂ than the sorghum (Table 7), implying that the ramps are better formed over the plant canopy. It is expected that the RSNR is higher over the sorghum where canopy drag and shear create an inflection point in the wind profile, promoting coherent structure generation (Antonia et al., 1979; Raupach et al., 1989). This is consistent with the observation by Paw U et al. (1992) that the relative strength of the ramp signal in the time series compared to background noise apparently increases when measurements are taken above taller canopies. For stable conditions, however, RSNR₁ and RSNR₂ are lower over the sorghum compared to the bare soil, and the mechanism behind this phenomenon is unclear. More investigation into the utility and limitations of the RSNR parameter is necessary and may lead to insights into coherent structure formation and new protocols for quality control of surface renewal measurements.

Regardless of surface and stability, RSNR₂ is consistently lower than the RSNR₁ (Table 7). The ramp characteristics of the Scale Two are resolved using a longer structure function lag compared to the lag used for resolving Scale One (Shapland et al., 2012a). The second-order structure function of turbulent noise increases with time lag because the energy associated with larger eddies

Table 7

Median ramp signal to noise ratio (RSNR) for the compensated 13 and 76 µm diameter thermocouples. The subscripts 1 and 2 correspond to Scale One (the smaller scale) and Scale Two (the larger scale), respectively.

Surface	Wire diameter (µm)	RSNR ₁		RSNR ₂	
		Unstable	Stable	Unstable	Stable
Bare soil	13	26.3	29.6	6.49	15.82
Bare soil	76	19.3	15.1	4.95	8.41
Sorghum	13	38.3	15.6	8.95	3.06
Sorghum	76	31.8	12.3	6.87	3.03

is greater (Kolmogorov, 1941). The increasing noise with increasing lag means the denominator in Eq. (14b) increases, resulting in a relatively low RSNR₂ compared to RSNR₁. This also may help explain the relatively low coefficients of determination observed in regressions comparing the Scale Two surface renewal flux to eddy covariance in contrast to the coefficients of determination in regressions comparing the Scale One surface renewal flux to eddy covariance (Shapland et al., 2012b). Alternative methods for estimating the ramp period at more than one scale that do not rely on ramp amplitude estimates may be helpful for improving surface renewal accuracy.

6. Conclusions

The alpha calibration converges to near to the theoretically predicted value of 0.5 once the frequency response characteristics of the thermocouple have been compensated. The convergent alpha calibration allows more accurate surface renewal sensible heat flux than previously possible without calibration against eddy covariance or other micrometeorological techniques. The findings in this paper represent a significant advance in the understanding of the surface renewal alpha calibration and the development of surface renewal as an inexpensive method for sensible heat flux density measurements. This paper also provides further support for the hypothesis that coherent structures are largely responsible for surface-layer fluxes.

Frequency response compensation is required for 76 and 25 μm thermocouples used in surface renewal sensible heat flux density measurements. The procedures described in this paper accurately compensate the frequency response limitations of 25 and 76 μm thermocouple signals. The compensation procedure enables the use of the more rugged thermocouples in surface renewal field experiments with both applied and theoretical objectives. For surface renewal flux estimates of other scalars such as carbon dioxide, the signal also should be corrected for the attenuation of the high frequency components prior to resolving the ramp characteristics.

The compensation procedure exaggerates the noise component of the signal. Regardless of ramp scale, the additional noise causes an overestimation of the ramp amplitude, an even greater overestimation of the ramp period, and therefore an underestimation in the ratio of the ramp amplitude to ramp period. Hence, the compensation procedure is broadly applicable for correcting thermocouple signals for both the surface renewal and eddy covariance flux measurements, but its accuracy for surface renewal measurements depends on the aspects of the site that influence coherent structure development and ramp formation. Nevertheless, the error stemming from the compensation procedure is within the range of error associated with micrometeorological measurements.

Acknowledgements

Partial support for this research was provided by J. Lohr Vineyards & Wines, the National Grape and Wine Institute, a NIFA Specialty Crops Research Initiative grant, and USDA-ARS CRIS funding (Research Project #5306-21220-004-00). The authors thank Mike Mata and Eric Kent for assistance with the field experiments, and Sam Matoba for assistance with the stage micrometer.

References

- Antonia, R.A., Chambers, A.J., Friehe, C.A., Van Atta, C.W., 1979. Temperature ramps in the atmospheric surface layer. *J. Atmos. Sci.* **36**, 99–108.
- Ballantyne, A., Moss, J.B., 1977. Fine wire thermocouple measurements of fluctuating temperature. *Comb. Sci. Technol.* **17**, 63–72.
- Bloomfield, P., 2000. Fourier Analysis of Time Series: An Introduction. Wiley, New York, 288 pp.
- Castellvi, F., 2004. Combining surface renewal analysis and similarity theory: a new approach for estimating sensible heat flux. *Water Resour. Res.* **40**, W05201.
- Chen, W., Novak, M.D., Black, T.A., 1997a. Coherent eddies and temperature structure functions for three contrasting surfaces. Part I: Ramp model with finite microfront time. *Boundary-Layer Meteorol.* **84**, 99–123.
- Chen, W., Novak, M.D., Black, T.A., 1997b. Coherent eddies and temperature structure functions for three contrasting surfaces. Part II: Renewal model for sensible heat flux. *Boundary-Layer Meteorol.* **84**, 125–147.
- Collis, D.C., Williams, M.J., 1959. Two-dimensional convection from heated wires at low Reynolds numbers. *J. Fluid Mech.* **49**, 357–389.
- Coulter, R.L., Wesely, M.L., 1980. Estimates of surface heat flux from sodar and laser scintillation measurements in the unstable boundary layer. *J. Appl. Meteorol.* **19**, 1209–1222.
- Duce, P., Spano, D., Snyder, R.L., 1997. Effect of different fine-wire thermocouple design on high frequency temperature measurement. In: AMS 23rd Conf. on Agricultural and Forest Meteorology, Albuquerque, NM, November 2–6, 1998, pp. 146–147.
- Gao, W., Shaw, R.H., Paw U, K.T., 1989. Observations of organized structure in turbulent flow within and above a forest canopy. *Boundary-Layer Meteorol.* **47**, 349–377.
- King, L.V., 1914. On the convection of heat from small cylinders in a stream of fluid. Determination of convection constants of small platinum wires with application to hot-wire anemometry. *Philos. Trans. A* **214**, 373–432.
- Kochendorfer, J., Meyers, T.P., Frank, J., Massman, W.J., Heuer, M.W., 2012. How well can we measure the vertical wind speed? Implications for fluxes of energy and mass. *Boundary-Layer Meteorol.* **145**, 383–398.
- Kolmogorov, A.N., 1941. Local structure of turbulence in an incompressible fluid for very large Reynolds numbers. *Dokl. Akad. Nauk SSSR* **30**, 299–303.
- Massman, W.J., Lee, X., 2002. Eddy covariance flux corrections and uncertainties in long-term studies of carbon and energy exchanges. *Agric. For. Meteorol.* **113**, 121–144.
- Massman, W.J., Clement, R., 2004. Chapter 4 – Uncertainty in eddy covariance flux estimates resulting from spectral attenuation. In: Lee, X., Massman, W.J., Law, B.E. (Eds.), *Handbook of Micrometeorology: A Guide for Surface Flux Measurement and Analysis*. Kluwer Academic Publishers, London, 250 pp.
- Mauder, M., Oncley, S.P., Vogt, R., Weidinger, T., Ribeiro, L., Bernhofer, C., Foken, T., Kohsieck, W., DeBruin, H.A.R., Liu, H., 2007. The energy balance experiment EBEX-2000. Part II: Intercomparison of eddy-covariance sensors and post-field data processing methods. *Boundary-Layer Meteorol.* **123**, 29–54.
- McBean, G.A., 1972. Instrument requirements for eddy correlation measurement. *J. Appl. Meteorol.* **11**, 1078–1084.
- McGee, T.D., 1988. *Principles and Methods of Temperature Measurement*. Wiley, New York, 581 pp.
- Monin, A.S., Obukhov, A.M., 1954. Basic laws of turbulent mixing in the ground layer of the atmosphere. *Izv. Akad. Nauk SSSR, Ser. Geofiz.* **151**, 163–187.
- Monin, A.S., Yaglom, A.M., 1975. *Statistical Fluid Mechanics*, vol. II. MIT Press, Cambridge, 874 pp.
- Moore, C.J., 1986. Frequency response corrections for eddy correlation systems. *Boundary-Layer Meteorol.* **37**, 17–35.
- Moratiel, R., Martinez-Cob, A., 2011. Evapotranspiration and crop coefficients of rice (*Oryza sativa* L.) under sprinkler irrigation in a semiarid climate determined by the surface renewal method. *Irrig. Sci.*, <http://dx.doi.org/10.1007/s00271-011-0319-8>.
- Paw U, K.T., Brunet, Y., Collineau, S., Shaw, R.H., Maitani, T., Qui, J., Hippis, L., 1992. On coherent structures in turbulence above and within agricultural plant canopies. *Agric. For. Meteorol.* **61**, 55–68.
- Paw U, K.T., Qiu, J., Su, H.-B., Watanabe, T., Brunet, Y., 1995. Surface renewal analysis: a new method to obtain scalar fluxes without velocity data. *Agric. For. Meteorol.* **74**, 119–137.
- Paw U, K.T., Snyder, R.L., Spano, D., Su, H.-B., 2005. Surface renewal estimates of scalar exchange. In: Hatfield, J.L. (Ed.), *Micrometeorology of Agricultural Systems*. American Society of Agronomy, Crop Science Society of America, Soil Science Society of America, pp. 455–483 (referred chapter).
- R Development Core Team, 2012. *R: A Language and Environment for Statistical Computing*. R Foundation for Statistical Computing, Vienna, ISBN 3-900051-07-0.
- Raupach, M.R., Finnigan, J.J., Brunet, Y., 1989. Coherent eddies in vegetation canopies. In: Proceedings Fourth Australasian Conference on Heat and Mass Transfer, Christchurch, New Zealand, 9–12 May, pp. 75–90.
- Reynolds, O., 1883. An experimental investigation of the circumstances which determine whether the motion of water shall be direct or sinuous, and of the law of resistance in parallel channels. *Philos. Trans. R. Soc.* **174**, 935–982.
- Scadron, M.D., Warshawsky, I., 1952. Experimental determination of time constants and Nusselt Numbers for Bare-wire thermocouples in high velocity air streams and analytical approximations of conduction and radiation errors. *NACA TN 2599*.
- Shapland, T.M., McElrone, A.J., Snyder, R.L., Paw U, K.T., 2012a. Structure function analysis of two-scale scalar ramps. Part I: Theory and modelling. *Boundary-Layer Meteorol.* **145**, 4–25.
- Shapland, T.M., McElrone, A.J., Snyder, R.L., Paw U, K.T., 2012b. Structure function analysis of two-scale scalar ramps. Part II: Ramp characteristics and surface renewal flux estimation. *Boundary-Layer Meteorol.* **145**, 27–44.
- Shapland, T.M., Snyder, R.L., Smart, D.R., Williams, L.E., 2012c. Estimation of actual evapotranspiration in winegrape vineyards located on hillside terrain using surface renewal analysis. *Irrig. Sci.* **30**, 471–484.

- Shapland, T.M., McElrone, A.J., Paw U, K.T., Snyder, R.L., 2012d. A turnkey logger program for field-scale energy flux density measurements using eddy covariance and surface renewal. *Ital. J. Agrometeorol.* 18, 5–16.
- Snyder, R.L., Spano, D., Paw U, K.T., 1996. Surface renewal analysis of sensible and latent heat flux density. *Boundary-Layer Meteorol.* 77, 249–266.
- Snyder, R.L., Paw U, K.T., Spano, D., Duce, P., 1997. Surface renewal estimates of evapotranspiration. *Short canopies. Acta Horticult.* 449, 49–55.
- Snyder, R.L., Spano, D., Duce, P., Baldocchi, D., Xu, L., Paw U, K.T., 2006. A fuel dryness index for grassland fire-danger assessment. *Agric. For. Meteorol.* 139, 1–11.
- Spano, D., Snyder, R.L., Duce, P., Paw U, K.T., 1997a. Surface renewal analysis for sensible heat flux density using structure functions. *Agric. For. Meteorol.* 86, 259–271.
- Spano, D., Duce, P., Snyder, R.L., Paw U, K.T., 1997b. Surface renewal estimates of evapotranspiration. *Tall canopies. Acta Horticult.* 449, 63–68.
- Spano, D., Snyder, R.L., Duce, P., Paw U, K.T., 2000. Estimating sensible and latent heat flux densities from grapevine canopies using surface renewal. *Agric. For. Meteorol.* 104, 171–183.
- Stull, R.B., 1988. *An Introduction to Boundary Layer Meteorology*. Kluwer Academic Publishers, Dordrecht, pp. 666 pp.
- Van Atta, C.W., 1977. Effect of coherent structures on structure functions of temperature in the atmospheric boundary layer. *Arch. Mech.* 29, 161–171.
- Wyngaard, J.C., Cote, O.R., Izumi, Y., 1971. Local free convection, similarity, and the budgets of shear stress and heat flux. *J. Atmos. Sci.* 28, 1171–1182.
- Wyngaard, J.C., Lemon, M.A., 1980. Behavior of the refractive index structure parameter in the entraining boundary layer. *J. Atmos. Sci.* 37, 1573–1585.
- Zapata, N., Martinez-Cob, A., 2001. Estimation of sensible and latent heat flux from natural sparse vegetation surfaces using surface renewal. *J. Hydrol.* 254, 215–228.